Published in final edited form as:
J Membr Biol. 2012 July ; 245(7): 369–380. doi:10.1007/s00232-012-9459-x.

Extracellular Loop Cysteine Mutant of Cx37 Fails to Suppress Proliferation of Rat Insulinoma Cells

Miranda E. Good, **José F. Ek-Vitorín**, and **Janis M. Burt**
Department of Physiology, University of Arizona, PO Box 245051, Tucson, AZ 85724, USA

Janis M. Burt: jburt@u.arizona.edu

Abstract

Although a functional pore domain is required for connexin 37 (Cx37)–mediated suppression of rat insulinoma (Rin) cell proliferation, it is unknown whether functional hemichannels would be sufficient or if Cx37 gap junction channels are required for growth suppression. To test this possibility, we targeted extracellular loop cysteines for mutation, expecting that the mutated protein would retain hemichannel, but not gap junction channel, functionality. Cysteines at positions 61 and 65 in the first extracellular loop of Cx37 were mutated to alanine and the mutant protein (Cx37-C61,65A) expressed in Rin cells. Although the resulting iRin37-C61,65A cells expressed the mutant protein comparably to Cx37 wild-type (Cx37-WT)–expressing Rin cells (iRin37), Cx37-C61,65A expression did not suppress the proliferation of Rin cells. As expected, iRin37-C61,65A cells did not form functional gap junction channels. However, functional hemichannels also could not be detected in iRin37-C61,65A cells by either dye uptake or electrophysiological approaches. Thus, failure of Cx37-C61,65A to suppress the proliferation of Rin cells is consistent with previous data demonstrating the importance of channel functionality to Cx37's growth-suppressive function. Moreover, failure of the Cx37-C61,65A hemichannel to function, even in low external calcium, emphasizes the importance of extracellular loop cysteines not only in hemichannel docking but also in determining the ability of the hemichannel to adopt a closed configuration that can open in response to triggers, such as low external calcium, effective at opening Cx37-WT hemichannels.

Keywords

Gap junction; Connexin; Hemichannel; Growth suppression; Insulinoma; Cx37

Introduction

Connexins, the protein products of the gap junction gene family, facilitate coordinated cell and tissue function by influencing and mediating intracellular, transmembrane and intercellular signaling. Intracellular signaling via connexins involves their interaction with a diverse array of proteins, the consequence of which can be regulated connexin function as well as regulation of intracellular signaling cascades (Kardami et al. 2007). The transmembrane signaling function of connexins is mediated by hemichannels (connexons). Hemichannels comprise a hexamer of connexin monomers that, when these channels are open, mediate transmembrane diffusion of ions and small molecules (Goodenough and Paul 2003). The intercellular signaling function of connexins is mediated by gap junction channels, which are formed when two hemichannels from neighboring cells dock to form an

Correspondence to: Janis M. Burt, jburt@u.arizona.edu.

intercellular channel that connects the cytosols of those cells. These gap junction channels support the diffusive exchange of ions and small molecules (Harris 2001). Although each connexin isoform is likely able to participate in intracellular, transmembrane and intercellular signaling, isoform-specific differences in their regulation as well as the signaling they mediate suggest the possible cell-and tissue-specific benefits of coexpressing multiple connexin isoforms (Sohl and Willecke 2004). Indeed, based on phenotypic differences in animals with connexin isoform deletion or substitution (Plum et al. 2000; Scherer et al. 1998; Simon et al. 1997), it is clear that connexins serve to facilitate the coordinated function of cells and the tissues they comprise in both a cell type and connexin isoform specific manner (Kardami et al. 2007).

Isoform and cell type specific growth suppression by connexins is well documented (e.g., Kardami et al. 2007; King and Bertram 2005), although the precise mechanisms underlying growth suppression by any given connexin are less clear. For example, connexin 37 (Cx37), but not Cx40 or Cx43, suppresses the proliferation of rat insulinoma (Rin) cells (Burt et al. 2008). A mutant form of Cx37 (Cx37-T154A) that does not form functional channels but retains the capacity to localize properly and form gap junction plaques, fails to suppress Rin cell proliferation, indicating that the capacity of Cx37 to form functional channels is necessary and the normal localization of the carboxyl terminus is insufficient for Cx37-mediated growth suppression of this cell type (Good et al. 2011). Since the T154A site likely renders both hemichannel and gap junction channel nonfunctional (Beahm et al. 2006), these studies leave unresolved which channel type is necessary for Cx37-mediated growth suppression.

Although the formation of gap junction channels depends upon the structural integrity of the extracellular loops, the formation of hemichannels does not (Foote et al. 1998). These loops share a high degree of sequence homology across connexin isoforms (Dahl et al. 1992; Nakagawa et al. 2010), with the six cysteines conserved in all gap junction–competent connexin isoforms (Sonntag et al. 2009). These cysteines are essential to the formation of functional gap junction channels, likely through interloop disulfide bond formation (Foote et al. 1998; Dahl et al. 1991, 1992). Specifically, disulfide bond formation between cysteines in the first and second extracellular loops, which occurs in a site- and position-specific manner, probably stabilizes the conformation of the extracellular domain such that proper docking of two hemichannels can occur (Foote et al. 1998). In Cx32, mutation of a single cysteine to serine was sufficient to prevent gap junction channel formation and function (Dahl et al. 1992). Bao and colleagues (2004) and more recently Tong and colleagues (2007) demonstrated that Cx43 with all six extracellular loop cysteines mutated to alanines fails to form functional gap junction channels but retains hemichannel function as determined by dye uptake. Together, these studies suggest that cells expressing a connexin with one or more of the cysteines in the extracellular loops mutated to alanine would be unable to form functional gap junction channels but would be able to form functional hemichannels.

In the current study we examined the functional consequences of mutating cysteine residues 61 and 65 in Cx37 to alanine (Cx37-C61,65A) on both the growth-suppressive and channel functions of Cx37. We demonstrate that Cx37-C61,65A does not suppress the proliferation of Rin cells, despite localizing to appositional and nonappositional membranes in a manner comparable to wild-type Cx37 (Cx37-WT) and Cx37-T154A. However, contrary to expectation, Cx37-C61,65A does not form functional hemichannels (or gap junction channels). Thus, consistent with previous data, the current results demonstrate that the growth-suppressive properties of Cx37 depend on the capacity of the protein to adopt a conformation able to support channel function.

Materials and Methods

Antibodies and Reagents

Reagents were purchased from Sigma-Aldrich (St. Louis, MO), except where noted. Anti-Cx37 antibody [αCx37-18264 (Simon et al. 2006)] was used for immunoblots and immunofluorescence. Secondary antibodies to anti-Cx37 antibody were horseradish peroxidase (HRP) conjugated to goat anti-rabbit antibodies (Amersham, Arlington Heights, IL) for immunoblotting and Cy3-conjugated anti-rabbit-IgG (Jackson ImmunoResearch, West Grove, PA) for immunofluorescence.

Mutant Connexin and Expression Vectors

Using the QuikChange Site-Directed Mutagenesis kit (Stratagene, San Diego, CA), the C61,65A mutation was introduced into the pTRE2h-mCx37 plasmid (Burt et al. 2008) using the following oligonucleotide primers (Operon Biotechnologies, Huntsville, AL): 5′-GCCCAGCCGGGCGCCACCAACGTCGCCTATGACCAGGC-3′ and 5′-CGGGTCGGCCCGCGGTGGTTGCAGCGGATACTGGTCCG-3′. Sequence was confirmed by the Genomic Analysis and Technology Core at the University of Arizona. The Cx37-WT and Cx37-C61,65A sequences were subcloned into the pcDNA3.1h vector

Cell Culture and Expression Vectors

iRin cells (Burt et al. 2008), cultured in RPMI 1640 medium supplemented with 10 % Fetal Plex (Gemini Bioproducts, Sacramento, CA), 300 μg/ml penicillin, 500 μg/ml streptomycin and 300 μg/ml G418 (GIBCO Invitrogen, Grand Island, NY), were transfected with the pTRE2h-mCx37-C61,65A plasmid using Lipofectamine (Invitrogen, Carlsbad, CA) and stably expressing cells selected by culturing in the same RPMI medium but also containing 100 μg/ml hygromycin. Clonal cell lines (iRin37-C61,65A) were isolated by dilution cloning. Connexindeficient MDCK cells [obtained from Paul Lampe (Solan and Lampe 2007)] were transiently transfected with either the Cx37WT or the Cx37-C61,65A sequence using the pcDNA3.1h vector. Cells were cultured in DMEM supplemented with 10 % Gem Cell Fetal Bovine Serum (Gemini Bioproducts). All cells were maintained at 37 °C in a humidified, 5 % CO_2 incubator.

Immunoblotting

Whole-cell protein was isolated as previously described (Burt et al. 2008), and protein concentration was determined using the BCA Assay (Pierce, Rockford, IL). Samples (50 μg of total protein) were loaded onto 12 % SDS-PAGE gels (Bio-Rad, Richmond, CA), electrophoresed and then transferred to nitrocellulose using the Trans-Blot Turbo Transfer System (Bio-Rad). Blots were blocked using 5 % nonfat dried milk. Enhanced chemiluminescence strategies, with SuperSignal West Dura and Femto Systems (mixed at a 2:1 ratio; Thermo Scientific, Waltham, MA), were used to visualize (Kodak Imagestation 2000; Kodak, Rochester, NY) connexin expression. Cx37 expression levels were quantified as previously described (Burt et al. 2001) by comparing sample band intensity to a standard curve generated with GST-Cx37 fusion protein (residues 233–329). This fusion protein runs as three distinct bands; their collective intensities were used to generate the standard curve.

Immunofluorescence

Cx37 localization was determined as previously described (Good et al. 2011). Briefly, iRin37 and iRin37-C61,65A cells, plated on glass coverslips and induced (2 μg/ml doxycycline) to express Cx37, were rinsed with divalent cation containing phosphate-buffered saline (PBS) and treated with 1 mM Sulfo-NHS-SS-Biotin (Thermo Scientific) to label lysine residues in the extracellular portions of membrane proteins. Excess biotin was

quenched with 100 mM glycine in PBS, and the cells were fixed in cold methanol and treated with 0.2 % Triton X-100 followed by 0.5 M NH_4Cl, each for 15 min. Cells were then rinsed with divalent cation-free PBS (DCF-PBS), blocked (in 4 % fish skin gelatin, 1 % normal goat serum and 0.1 % Triton X-100 in DCF-PBS) and exposed to primary antibody for 2 h. After rinsing, secondary antibodies were applied (Cy3-conjugated, diluted 1:200 in blocking reagent for Cx37; Cy5-conjugated streptavidin, diluted 1:250 in blocking reagent, for detection of biotinylated surface proteins). Labeled proteins were visualized with a Zeiss (Thornwood, NY) LSM510meta-NLO confocal/multiphoton fluorescence microscope (lasers set at 514 nm for Cy3 and 633 nm for Cy5 detection).

MDCK cells, plated at low density, were transfected with pcDNA3.1h-mCx37 or pcDNA3.1h-mCx37-C61,65A using Lipofectamine and 24 h later processed as described for labeling and visualization of Cx37.

Immunoprecipitation of Surface Biotinylated Proteins

Subconfluent cells induced to express Cx37 were rinsed with either PBS or DCF-PBS and treated with 10 mM dithiothreitol (DTT) in PBS or DCF-PBS for 20 min at room temperature. Cells in DCF-PBS were rinsed with EGTA-supplemented (5 mM) external solution [in mM: 142.5 NaCl, 4 KCl, 1 $MgCl_2$, 5 glucose, 2 sodium pyruvate, 10 HEPES, 15 CsCl, 10 TEACl, 1 $CaCl_2$ (pH 7.2), 320 mOsM] and rinsed again with DCF-PBS. These cells and those not exposed to low-Ca^{2+} washes (in PBS) were then incubated in 0.5 mg/ml maleimide-PEG_2-biotin (Thermo Scientific) in PBS or DCF-PBS, as appropriate, for 1 h at 4 °C on a rotator. After quenching excess biotin with 100 mM glycine (in PBS or DCF-PBS), cell protein was harvested with immunoprecipitation (IP) buffer [containing 150 mM NaCl, 10 mM Tris HCl, 1 % Triton X-100, 1 % Na deoxycholate, 0.1 % SDS and a protease inhibitor cocktail tablet (catalog no. 11836153001, Roche, Indianapolis, IN; pH 6.8), pH 7.4]. Streptavidin-coupled resin (Thermo Scientific) preequilibrated in IP buffer was added to harvested cell protein and incubated overnight at 4 °C. The mixture was centrifuged (2,500×*g* for 15 s at 4 °C) and the resin washed three times with cold IP buffer and once with PBS. Resin-coupled proteins were then resuspended in sample buffer (100 mM Tris, 4 % SDS, 10 % glycerol, 5 mM NaF, 0.25 mM Na_3VO_4, 2 mM PMSF and 0.02 % bromophenol blue with added protease inhibitor cocktail, pH 6.8), boiled, vortexed and centrifuged (15,000×*g* for 1 min); and the immunoprecipitated proteins were electrophoretically separated [25 μl per sample, 12 % SDS-PAGE gels (Bio-Rad)] and immunoblotted for Cx37 expression, as described above.

Proliferation

As previously described (Burt et al. 2008; Good et al. 2011), iRin37 or iRin37-C61,65A cells were plated at an initial density of 3×10^4/well in six-well plates. 24 h after plating (day zero of proliferation curve), cells were induced (dox+) or not (dox−) with 2 μg/ml doxycycline. Medium was refreshed every 48 h (with or without added doxycycline, as appropriate). Triplicate wells were harvested and counted (Cellometer Auto T4; Nexcelom Bioscience, Lawrence, MA) every 3 days over a 21-day period.

Dye-Uptake Studies

iRin37 or iRin37-C61,65A clone 1C3 cells were plated at low density and induced or not for 24–48 h. Cells were rinsed with medium, external solution and external solution containing 5 mM EGTA. Two rings [made from the tops of 14-ml BD Falcon (Franklin Lakes, NJ) tubes] were adhered to the dish with Vaseline, creating two wells; dye was added to each well, and the dish was placed on ice and protected from ambient light. The dye solution contained 1.25 mg/ml *N,N,N*-trimethyl-2-[methyl-(7-nitro-2,1, 3-benzoxadiol-4-yl)amino]ethanaminium (NBD-M-TMA) (Bednarczyk et al. 2000) and 0.125 mg/ml

tetramethyl-rhodamine dextran (rhodamine, molecular weight 3,000; Molecular Probes, Eugene, OR) added to Ca-free external solution supplemented or not with 5 mM EGTA. Dye and the rings were removed after a 15-min dye-uptake period, and cells were rinsed with culture medium followed by external solution. Cells were imaged with an Olympus (Tokyo, Japan) IX71 or BX50WI fluorescence microscope; differential interference contrast (DIC) and fluorescence images of multiple fields within each ringed area of cells were acquired [CoolSnap ES camera (Photometrics, Tucson, AZ) and V++ software (Digital Optics, Auckland, New Zealand); 41001HQ filter for imaging NBD-M-TMA and U-MWIGA3 filter for imaging rhodamine (both from Olympus)]. Each set of images was scored for NBD-M-TMA-positive and rhodamine-dextran-negative cells and the total number of cells. Multiple fields were imaged for each well. Totals from each field within a well were combined to calculate a percent NBD-M-TMA-positive value. We performed *t*-tests on the dox+ versus dox− groups.

Electrophysiology

iRin parental, iRin37 or iRin37-C61,65A cells were plated onto glass coverslips at low densities such that single cells and cell pairs predominated. One hour after plating doxycycline (2 μg/ml) was added or not to the cells, and 24–48 h later junctional (cell pairs) or membrane (single cells) conductance was evaluated. Coverslips were placed in a custom-made chamber and bathed in external solution. Patch pipettes were fabricated as previously described (Burt et al. 2008; Ek-Vitorín and Burt 2005) and back-filled with internal solution (in mM: 124 KCl, 14 CsCl, 9 HEPES, 9 EGTA, 0.5 $CaCl_2$, 5 glucose, 9 TEACl, 3 $MgCl_2$, 5 Na_2ATP).

Junctional and single gap junction channel conductances were measured as previously described (Burt et al. 2008; Ek-Vitorín and Burt 2005), using either discontinuous single electrode voltage clamp (NPI SEC-05LX) or traditional patch-clamp (Axopatch 1D) amplifiers. In either case, transjunctional voltages (V_j) of 25–50 mV (non-pulsed cell held at 0 mV, while the pulsed cell was clamped to the indicated membrane potential) were applied to reveal the activity of Cx37 gap junction channels.

Hemichannel data were collected in single whole-cell voltage-clamp configuration; depolarizing or hyperpolarizing voltage ramps (between +50 or +100 and −100 mV, 7 s) or square pulses of variable magnitude and duration were applied. Ramps were run every 15–20 s over a period of 5–40 min. Typically, steady transmembrane potentials were continuously applied (10–40 min), with only short interruptions to evince the baseline. The longer recordings were performed while exchanging the external solution (at least twice the chamber volume over 1–2 min); thus, any event appearing while lowering external calcium was likely captured.

Results

To determine whether functional hemichannels would be sufficient to support Cx37-mediated growth suppression, we mutated two of the three cysteines in the first extracellular loop of Cx37 to alanines, with the expectation that the mutant protein would be unable to form functional gap junction channels but retain its ability to form functional hemichannels. Three hygromycin-resistant iRin37-C61,65A subclones (1B3, 1C3 and 1D2) were selected for further study. Cx37 expression levels in these subclones were comparable to that observed in iRin37 cells (Fig. 1A).

Since we previously demonstrated that channel function was necessary for Cx37-mediated growth suppression, we next determined, using two approaches, whether the Cx37-C61,65A protein localized to the plasma membrane in a manner comparable to Cx37-WT. First,

immunofluorescence and confocal microscopy were used to examine the localization of WT and mutant Cx37 in both iRin cells and transiently transfected MDCK cells. iRin37 and iRin37-C61,65A clone 1C3 and 1D2 cells (Fig. 1B, panels a, b and c, respectively) induced for 24 h with 2 μg/ml doxycycline revealed Cx37 expression in the cytoplasm and as punctate and diffuse labeling at appositional and nonappositional plasma membranes (arrows). Similarly, Cx-deficient MDCK cells transiently transfected to express Cx37-WT or Cx37-C61,65A (Fig. 1B, panels d and e, respectively) expressed Cx37 in the cytoplasm and both appositional and nonappositional plasma membrane. Second, biotin-coupled maleimide was used to label reactive cysteines exposed (by DTT treatment in the presence or absence of extracellular calcium) on the extracellular surface of Cx37-WT- and Cx37-C61,65A-expressing cells. Biotinylated protein was immunoprecipitated from total protein with streptavidin-conjugated resin and Cx37 protein detected by immunoblotting. Cx37 was detected with this strategy in both the WT and mutant-expressing cell lines (Fig. 1C), indicating that both the WT and Cx37-C61,65A proteins were present in the plasma membrane. Together, the immunofluorescence and biotinylation results indicated that both proteins (mutant and WT) localize to and insert into the plasma membrane.

Next, we determined whether expression of the Cx37-C61,65A protein altered the proliferative properties of iRin cells. The noninduced cells of all cell lines proliferated comparably (Fig. 2A). When iRin37 cells were induced to express Cx37-WT, proliferation over the 21-day period was significantly suppressed (Fig. 2B). In contrast, induced expression of Cx37-C61,65A had no effect on Rin cell proliferation (Fig. 2B), even in the 1D2 clone with the highest level of expression. These results are similar to those obtained with the Cx37-T154A mutant (Good et al. 2011), which eliminates Cx37's growth-suppressive properties and, demonstrably, junctional channel formation. We therefore questioned whether Cx37-C61,65A formed functional hemichannels.

Initially, we determined whether the Cx37-C61,65A protein formed functional hemichannels using a dye-uptake strategy. Cx37 gap junction channels are cation-selective and readily permeated by the small cationic dye NBD-M-TMA^+ (Ek-Vitorín and Burt 2005), so this dye was selected to determine whether Cx37-C61,65A hemichannels would mediate dye uptake. A gap junction channel–impermeant dye (3,000-dalton rhodamine-labeled dextran) was included in all uptake experiments so that damaged cells (positive for rhodamine) would not be mistakenly counted as positive for hemichannel-mediated dye uptake. After washing Cx37-WT-expressing iRin cells with an EGTA–low-Ca^{2+} solution and performing the dye-uptake experiment in a low-[Ca^{2+}] dye solution, many more induced iRin37 cells were positive for NBD-M-TMA^+ than noninduced cells (compare panels a, b and c in Fig. 3B to panels d, e and f). Data from multiple experiments (quantified in Fig. 3A) showed that approximately 43 ± 4 % of Cx37-WT-expressing iRin cells (n = 8 wells) were positive for NBD-M-TMA^+ uptake and negative for rhodamine-dextran, a value significantly (p < 0.001) larger than the 10 ± 4 % observed for noninduced cells (n = 7 wells). Repetition of these procedures on induced versus noninduced iRin37-C61,65A cells (clone 1C3) revealed no significant differences in dye-positive cells (compare panels g, h and i in Fig. 3B to panels j, k and l). Of induced iRin-Cx37-C61,65A cells (n = 10 wells), 6 ± 1 % were NBD-M-TMA^+ positive compared to 6 ± 2 % of noninduced cells (n = 9 wells) (Fig. 3A). These results suggest that Cx37-C61,65A does not form a functional hemichannel; however, the dye-uptake approach is insensitive to the activity of dye-impermeant channels and to activity of individual channels, so we next turned to electrophysiological approaches.

To facilitate recognition of possible Cx37-C61,65A channel events, we first characterized the channels present in iRin parental cells and the channels formed by Cx37-WT. Parental iRin cells do not form functional gap junctions (data not shown). Using dual whole-cell voltage-clamp methods, the mean macroscopic conductance observed for induced iRin37

cells was 4 ± 1 nS (n = 13, including two cell pairs that showed no measurable coupling) (Fig. 4A). This level of coupling is comparable to previously reported data for this cell line (Burt et al. 2008; Good et al. 2011). In contrast, no electrical coupling could be detected in either induced (n = 19) or noninduced (n = 9) iRin37-C61,65A-expressing cells (Fig. 4A)—all values were below 0.3 nS and not different from system noise levels. Large-conductance single-channel events were observed in iRin37 cell pairs with naturally low coupling levels (Fig. 4B). In solutions containing 1 mM Ca^{2+} (Fig. 4B), gap junction channel events were between 250 and 350 pS and dwell times at any conductance level were very brief (flickering activity). In contrast, when in low $[Ca^{2+}]_0$ (Fig. 4C) channel conductances were larger, residual states evident and dwell times longer. As expected, comparable junctional channel activity was not seen in iRin37-C61,65A-expressing cell pairs (n = 19), indicating that this mutant does not form functional gap junction channels.

Based on the behavior of the Cx37-WT gap junction channel, hemichannel conductances were expected to be quite large (500–700 pS, double the gap junction channel's conductance). Most voltage ramps performed on single Cx37-WT-expressing cells under normal external calcium conditions revealed no evidence of channel activity, but some showed activity at voltages incompatible with activity of Cx37-WT hemichannels, V_m > ±70 mV; the presence of these channels was confirmed and their amplitude (75–100 pS) documented with square pulses of V_m > ±70 mV (data not shown). Channels similar to these were also frequently observed in iRin parental cells (not transfected with any connexins) (Fig. 5A, B) and in both induced and noninduced iRin37-C61,65A cells (Fig. 5E, F). Thus, these events are unlikely to represent Cx37 hemichannel activity. On occasion (one in seven tested cells), voltage ramps performed in normal $[Ca^{2+}]_0$ on Cx37-WT-expressing cells revealed, transiently, activity in a V_m range (±20–50 mV) compatible with the opening of Cx37-WT hemichannels (Fig. 5C). Accordingly, in Cx37-WT-expressing cells, large-conductance (≥300 pS) transitions were observed during application of small V_m pulses (Fig. 5D) (one cell out of four tested, two successive pulses of many applied over more than 20 min in normal calcium). No similar activity was observed during either voltage ramps (n = 28 cells, Fig. 5E) or application of square pulses (n = 7 cells, recording from 10 to >25 min long; Fig. 5F) performed on Cx37-C61,65A mutant–expressing cells.

Since dye-uptake studies were successful only when the cells were washed with an EGTA-containing solution, we examined both Cx37-WT- and Cx37-C61,65A-expressing cells for electrophysiological evidence of hemichannel activity following a similar protocol. Hemichannel openings were transiently seen in two out of ten successive ramps implemented immediately following the lowering of external calcium with EGTA-containing solution in a Cx37-WT-expressing cell (Fig. 6A). In three out of six additional cells, similar, although shorter, duration openings were documented 5–20 min after lowering $[Ca^{2+}]_0$ (not shown). Hemichannel transitions of Cx37-WT were also seen under these low-$[Ca^{2+}]_0$ conditions during application of small V_m square pulses (channels transiently present within the first 5 min after lowering $[Ca^{2+}]_0$ in two of four cells; 20- to 30-min recordings; Fig. 6B). In contrast, comparable hemichannel activity was not observed in Cx37-C61,65A-expressing cells during application of ramps (six cells, 25- to 50-min records) or square pulses (five cells, 30- to 45-min records) in low $[Ca^{2+}]_0$ (Fig. 6C, D). Together the electrophysiology data strongly suggest either that Cx37-C61,65A does not form a functional hemichannel or that its open probability is sufficiently low under the conditions of our measurements that we could not detect it.

Discussion

Connexins form channels that serve (at least) two functions, transmembrane and intercellular signaling. In both cases the channels mediate the diffusive flux of ions and

small molecules down their electrochemical gradients. While channel function is the best-described function of connexins, it is increasingly clear that the carboxy terminus of these proteins, through interaction with an array of intracellular proteins, also participates in cellular functions in a channel-independent manner. Several connexins have been demonstrated to participate in tumor suppression via both channel-dependent and channel-independent mechanisms (Kardami et al. 2007; King and Bertram 2005). We previously demonstrated that in Rin cells Cx37, but not Cx40 or Cx43, suppresses cell proliferation by prolonging all phases of the cell cycle, G_1 most prominently (Burt et al. 2008). To understand which properties of Cx37 are central to its growth-suppressive action, we first explored whether channel function was necessary for Cx37-mediated growth suppression. Since Cx40 and Cx43 form channels with a similar or less selective permeability profile than Cx37 (Ek-Vitorín and Burt 2005; Weber et al. 2004), we expected that channel function would not be necessary for Cx37-mediated growth suppression. Contrary to expectation, Cx37-T154A, which forms a nonfunctional gap junction channel, was not growth-suppressive, suggesting that channel functionality is necessary for Cx37-mediated growth suppression in Rin cells (Good et al. 2011). Although we did not test this mutant for hemichannel function, mutation of the corresponding highly conserved site in Cx50 renders both the hemichannel and gap junction channel nonfunctional (Beahm et al. 2006); thus, it is probable that Cx37-T154A hemichannels are also nonfunctional. Thus, the Cx37-T154A study did not permit us to discern whether functionality of hemichannels, gap junction channels or both is necessary for Cx37-mediated growth suppression.

In the current study we attempted to address the sufficiency of hemichannels in Cx37-mediated growth suppression, expecting that functional hemichannels would be sufficient and functional gap junction channels unnecessary for Cx37-mediated growth suppression. Three observations lead to this hypothesis. First, Cx37-WT-expressing Rin cells are growth-suppressed at all tested plating densities, even densities where cell–cell contact and, therefore, gap junction formation are rare (Burt et al. 2008). Second, Cx37 hemichannels appear to be functional under physiological conditions, at least in some cell types (Wong et al. 2006). Third, transmembrane gradients for ions and small molecules (e.g., calcium and ATP) are always present, whereas intercellular gradients are only transiently present because gap junction channels, by mediating diffusive exchange, tend to neutralize these gradients. Thus, opening of Cx37-WT hemichannels could mediate efflux or influx of critical signaling molecules that directly or indirectly regulate intracellular signaling processes involved in cell cycle progression.

To address whether Cx37 hemichannels might be sufficient to explain Cx37-mediated growth suppression, we created a mutant that we expected would support hemichannel activity comparable to that displayed by Cx37-WT but not support gap junction channel formation. Available evidence suggested that mutation of one or more of the six highly conserved cysteines located in the extracellular loops of connexins would disable gap junction channel formation while preserving hemichannel functionality (Foote et al. 1998; Dahl et al. 1991, 1992; Bao et al. 2004; Tong et al. 2007). Consequently, we mutated the second and third cysteines in the first extracellular loop of Cx37 to alanines and stably transfected the encoding sequence into iRin cells, thereby creating the iRin37-C61,65A cell lines. Cx37 expression, localization to and insertion into the plasma membrane were comparable in iRin37-C61,65A and iRin37 cells. However, unlike the wild-type protein, the Cx37-C61,65A protein did not suppress the proliferation of iRin cells.

Failure of Cx37-C61,65A to growth-suppress prompted us to check whether the mutated protein formed functional hemichannels but nonfunctional gap junction channels. Cells expressing Cx37-C61,65A were never observed to take up NBD-M-TMA^+, a dye previously shown to readily permeate Cx37-WT gap junction channels (Ek-Vitorín and Burt 2005) and

shown here to be taken up by iRin37 cells only when induced to express Cx37-WT protein and exposed to low-$[Ca^{2+}]_0$ conditions. In addition, using whole-cell voltage-clamp techniques, we detected functional Cx37-WT hemichannels and gap junction channels in both normal and low-$[Ca^{2+}]_0$ conditions but were unable to detect functional Cx37-C61,65A hemichannels or gap junction channels under comparable recording conditions. Thus, the failure of Cx37-C61,65A to suppress proliferation of Rin cells is entirely consistent with our previous studies demonstrating that channel functionality is necessary and proper localization of a normal carboxy terminus insufficient for Cx37-mediated growth suppression.

Failure of Cx37-C61,65A to form functional hemichannels suggests either that disruption of disulfide bond formation in the extracellular loops prevents the channel from adopting a (closed) configuration that can be triggered to open (by docking, exposure to low $[Ca^{2+}]_0$, mechanical stimulus or even phosphorylation-dependent regulation) or that the open configuration is blocked by the extracellular loops due to mutations there. Arguing against the possibility of channel block is the complete absence of hemichannel events and dye uptake in cells expressing the mutant protein, even when “triggered” to open by exposure to low-$[Ca^{2+}]_0$ conditions. Bao and colleagues (2004) and Tong and colleagues (2007) reported that Cx43 with all six cysteines in the extracellular loops mutated to alanine forms functional hemichannels with Ca^{2+}-sensitive open probability characteristics. Assuming similar behavior of other connexins, these observations collectively suggest that docking of hemichannels to form functional gap junction channels is blocked by mutation of even one cysteine in the extracellular loops (Dahl et al. 1992; Foote et al. 1998); and our data suggest that mutation of fewer than all six cysteines results in hemichannels that are closed and unable to be triggered open.

We expected the current study to distinguish whether Cx37 hemichannel activity, not gap junction channel activity, was sufficient to explain Cx37-mediated growth suppression of Rin cells and instead provide further evidence that an open channel configuration must be possible for growth suppression by Cx37 (Burt et al. 2008; Good et al. 2011). It remains unclear what, if anything, permeates the hemichannel/gap junction channel to influence cell cycle progression. Potentially germane to this issue, however, is the observation that the wild-type hemichannel opens in the presence of extracellular calcium ions, albeit with only modest probability. However, since culture medium contains “normal” levels of calcium and Cx37 is growth-suppressive at cell densities where gap junction channel formation is rare (Burt et al. 2008), hemichannels able to open could allow the influx (or efflux) of signaling molecules with a growth-regulatory effect.

In summary, we have demonstrated that mutation of the second and third cysteines in the first extracellular loop of Cx37 to alanines results in a protein that is no longer growth-suppressive to Rin cells. The absence of a growth-suppressive function is consistent with previous observations in which the capacity to form a functional channel was demonstrated as necessary for the growth-suppressive action of Cx37. Our data further suggest that disulfide bond formation between the extracellular loops is critical to the hemichannel’s ability to adopt a conformation able to be triggered open as well as its ability to dock with another hemichannel to form a gap junction channel. Alternate (or additional) mutation sites will be necessary to create a Cx37 protein able to form functional hemichannels but unable to form functional gap junction channels. Thus, it remains to be determined whether transmembrane (hemichannel) or intercellular (gap junction channel) signaling, or both, is necessary for Cx37-mediated growth suppression and whether channel-independent properties of Cx37 might also be necessary.

Acknowledgments

The authors acknowledge Dr. Ross Johnson for encouraging, in a hands-on manner and from a distance, our pursuit of hemichannel function. The authors also acknowledge the technical support of Tasha K. Nelson. These studies were supported by the National Institutes of Health, grants (to J.M.B.) R01HL057832, R01HL077675 and T32HL007249 (supporting M.E.G.).

References

Bao X, Chen Y, Reuss L, Altenberg GA. Functional expression in *Xenopus* oocytes of gap-junctional hemichannels formed by a cysteine-less connexin 43. J Biol Chem. 2004; 279:9689–9692. [PubMed: 14676187]

Beahm DL, Oshima A, Gaietta GM, Hand GM, Smock AE, Zucker SN, Toloue MM, Chandrasekhar A, Nicholson BJ, Sosinsky GE. Mutation of a conserved threonine in the third transmembrane helix of alpha- and beta-connexins creates a dominant-negative closed gap junction channel. J Biol Chem. 2006; 281:7994–8009. [PubMed: 16407179]

Bednarczyk D, Mash EA, Aavula BR, Wright SH. NBD-TMA: a novel fluorescent substrate of the peritubular organic cation transporter of renal proximal tubules. Pflugers Arch. 2000; 440:184–192. [PubMed: 10864014]

Burt JM, Fletcher AM, Steele TD, Wu Y, Cottrell GT, Kurjiaka DT. Alteration of Cx43:Cx40 expression ratio in A7r5 cells. Am J Physiol Cell Physiol. 2001; 280:C500–C508. [PubMed: 11171569]

Burt JM, Nelson TK, Simon AM, Fang JS. Connexin 37 profoundly slows cell cycle progression in rat insulinoma cells. Am J Physiol Cell Physiol. 2008; 295:C1103–C1112. [PubMed: 18753315]

Dahl G, Levine E, Rabadan-Diehl C, Werner R. Cell/cell channel formation involves disulfide exchange. Eur J Biochem. 1991; 197:141–144. [PubMed: 1707811]

Dahl G, Werner R, Levine E, Rabadan-Diehl C. Mutational analysis of gap junction formation. Biophys J. 1992; 62:172–180. [PubMed: 1376165]

Ek-Vitorín JF, Burt JM. Quantification of gap junction selectivity. Am J Physiol Cell Physiol. 2005; 289:C1535–C1546. [PubMed: 16093281]

Foote CI, Zhou L, Zhu X, Nicholson BJ. The pattern of disulfide linkages in the extracellular loop regions of connexin 32 suggests a model for the docking interface of gap junctions. J Cell Biol. 1998; 140:1187–1197. [PubMed: 9490731]

Good ME, Nelson TK, Simon AM, Burt JM. A functional channel is necessary for growth suppression by Cx37. J Cell Sci. 2011; 124:2448–2456. [PubMed: 21693589]

Goodenough DA, Paul DL. Beyond the gap: functions of unpaired connexon channels. Nat Rev Mol Cell Biol. 2003; 4:285–294. [PubMed: 12671651]

Harris AL. Emerging issues of connexin channels: biophysics fills the gap. Q Rev Biophys. 2001; 34:325–472. [PubMed: 11838236]

Kardami E, Dang X, Iacobas DA, Nickel BE, Jeyaraman M, Srisakuldee W, Makazan J, Tanguy S, Spray DC. The role of connexins in controlling cell growth and gene expression. Prog Biophys Mol Biol. 2007; 94:245–264. [PubMed: 17462721]

King TJ, Bertram JS. Connexins as targets for cancer chemoprevention and chemotherapy. Biochim Biophys Acta. 2005; 1719:146–160. [PubMed: 16263076]

Nakagawa S, Maeda S, Tsukihara T. Structural and functional studies of gap junction channels. Curr Opin Struct Biol. 2010; 20:423–430. [PubMed: 20542681]

Plum A, Hallas G, Magin T, Dombrowski F, Hagendorff A, Schumacher B, Wolpert C, Kim J-S, Lamers WH, Evert M, Meda P, Traub O, Willecke K. Unique and shared functions of different connexins in mice. Curr Biol. 2000; 10:1083–1091. [PubMed: 10996788]

Scherer SS, Xu YT, Nelles E, Fischbeck K, Willecke K, Bone LJ. Connexin32-null mice develop demyelinating peripheral neuropathy. Glia. 1998; 24:8–20. [PubMed: 9700485]

Simon AM, Goodenough DA, Li E, Paul DL. Female infertility in mice lacking connexin 37. Nature. 1997; 385:525–529. [PubMed: 9020357]

Simon AM, Chen H, Jackson CL. Cx37 and Cx43 localize to zona pellucida in mouse ovarian follicles. Cell Commun Adhes. 2006; 13:61–77. [PubMed: 16613781]

Sohl G, Willecke K. Gap junctions and the connexin protein family. Cardiovasc Res. 2004; 62:228–232. [PubMed: 15094343]

Solan JL, Lampe PD. Key connexin 43 phosphorylation events regulate the gap junction life cycle. J Membr Biol. 2007; 217:35–41. [PubMed: 17629739]

Sonntag S, Sohl G, Dobrowolski R, Zhang J, Theis M, Winterhager E, Bukauskas FF, Willecke K. Mouse lens connexin23 (Gje1) does not form functional gap junction channels but causes enhanced ATP release from HeLa cells. Eur J Cell Biol. 2009; 88:65–77. [PubMed: 18849090]

Tong D, Li TY, Naus KE, Bai D, Kidder GM. In vivo analysis of undocked connexin43 gap junction hemichannels in ovarian granulosa cells. J Cell Sci. 2007; 120:4016–4024. [PubMed: 17971414]

Weber PA, Chang HC, Spaeth KE, Nitsche JM, Nicholson BJ. The permeability of gap junction channels to probes of different size is dependent on connexin composition and permeant-pore affinities. Biophys J. 2004; 87:958–973. [PubMed: 15298902]

Wong CW, Christen T, Roth I, Chadjichristos CE, Derouette JP, Foglia BF, Chanson M, Goodenough DA, Kwak BR. Connexin37 protects against atherosclerosis by regulating monocyte adhesion. Nat Med. 2006; 12:950–954. [PubMed: 16862155]

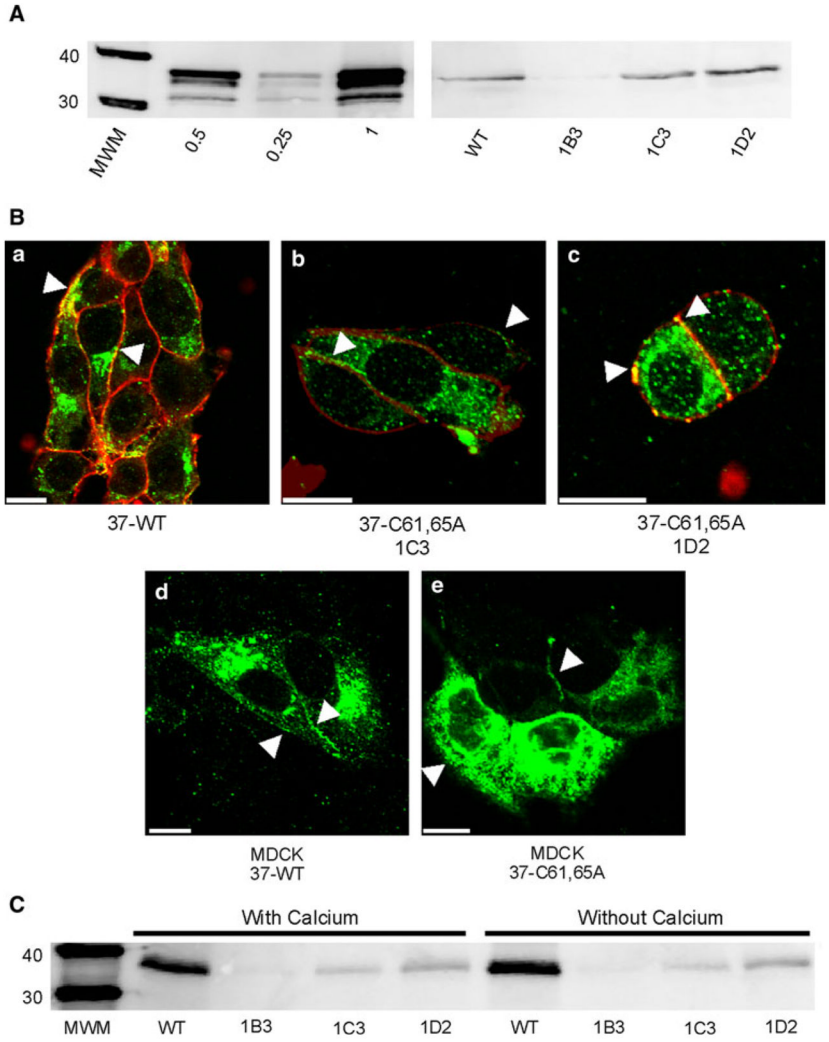

Fig. 1.

Expression and localization of Cx37-C61,65A and Cx37-WT are comparable. **A** Western blots of GST-37CT loaded in different amounts (*left*) and total protein isolated from iRin37 and three clones (1B3, 1C3 and 1D2) of iRin37-C61,65A cells (*right*). iRin cells were induced for 24 h with 2 μg/ml doxycycline, whole-cell protein was isolated and 50 μg of total cell protein was loaded for each sample. Expression levels for each cell line, determined by comparing band intensities of the samples to the standard curve generated using GST-37CT, were 3.7, 4.5 and 5.1 pmol/mg of total cell protein for clones 1B3, 1C3 and 1D2, respectively, and 4.5 pmol/mg protein for iRin37 cells. **B** Confocal images of Cx37 (*green*) localization with biotinylated membrane proteins (*red*) in induced iRin37 (37-WT) (*a*), iRin37-C61,65A 1C3 (37-C61,65A 1C3) (*b*) and iRin37-C61,65A 1D2 (37-C61,65A 1D2) (*c*) cells showing the presence of punctate labeling at appositional and nonappositional membranes (*arrows*). Confocal images of Cx37 (*green*) localization in MDCK cells transiently transfected to express Cx37-WT (MDCK 37-WT) (*d*) or Cx37-C61,65A (MDCK 37-C61,65A) (*e*) also showing the presence of punctate labeling at appositional and nonappositional membranes (*arrows*). *Scale bars* = 10 μm. **C** Western blot of membrane localized Cx37 isolated from Cx37-WT or -C61,65A expressing iRin cells. Induced iRin37 (WT) and iRin37-C61,65A clones 1B3, 1C3 and 1D2 were DTT- and maleimide-biotin-treated and harvested, and protein was immunoprecipitated with

streptavidin and immunoblotted with anti-Cx37 antibody. Solutions either contained or lacked calcium. Detected Cx37 indicates membrane insertion of this protein. Differences in band intensity in part reflect different cell densities in initial samples. Loaded 25 μl of each sample

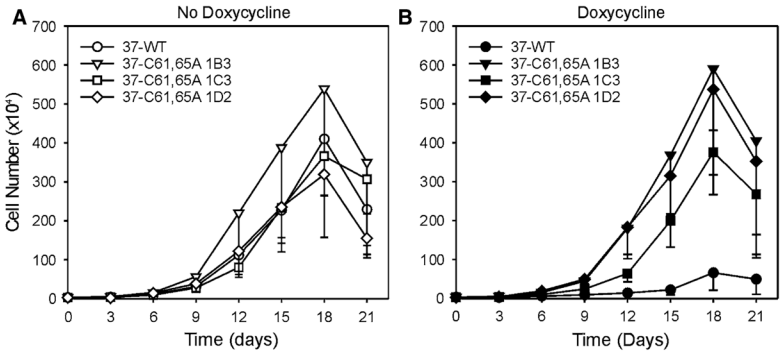

Fig. 2.

Proliferation of Rin cells is suppressed by expression of Cx37-WT but not Cx37-C61,65A. **A** Proliferation was comparable between iRinCx37-WT and the three clones of iRinCx37-C61,65A when connexin expression was not induced. In contrast, proliferation of induced iRinCx37-WT cells (*filled circles*, **B**) was suppressed compared to the iRin clones with induced expression of Cx37-C61,65A. Four growth curves (with or without dox) were performed for each cell line except the iRin37-C61,65A-1C3 clone, for which five experiments were performed. Where *error bars* are not obvious, they are smaller than the size of the data point

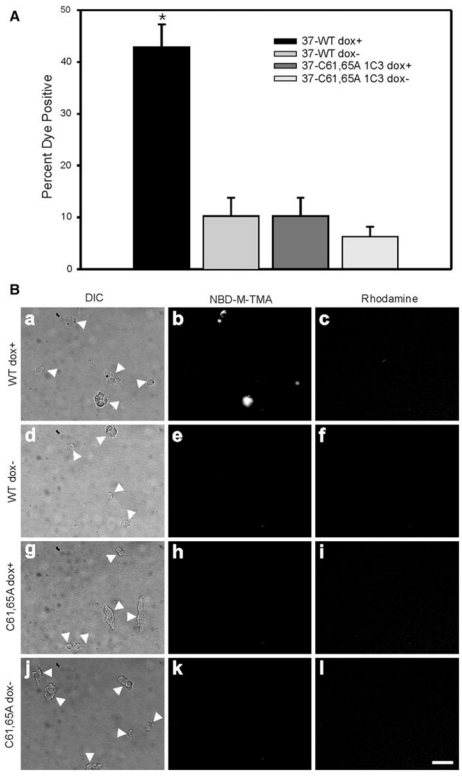

Fig. 3.

Cx37-C61,65A does not form hemichannels able to mediate dye uptake. **A** The percent of cells positive for NBD-M-TMA uptake and negative for rhodamine dextran was compared to determine hemichannel function. In cells induced to express Cx37-WT, dye uptake was significantly more frequent (*$p < 0.001$) than in noninduced cells or cells induced to express Cx37-C61,65A. **B** Representative images of DIC (*arrows* indicate isolated cells or cell clusters), NBD-M-TMA and rhodamine dextran fields for iRin37 induced (*a–c*) and noninduced (*d–f*), iRin37-C61,65A 1C3 induced (*g–i*) and noninduced (*j–l*). *Scale bar* = 20 μm, applies to all images

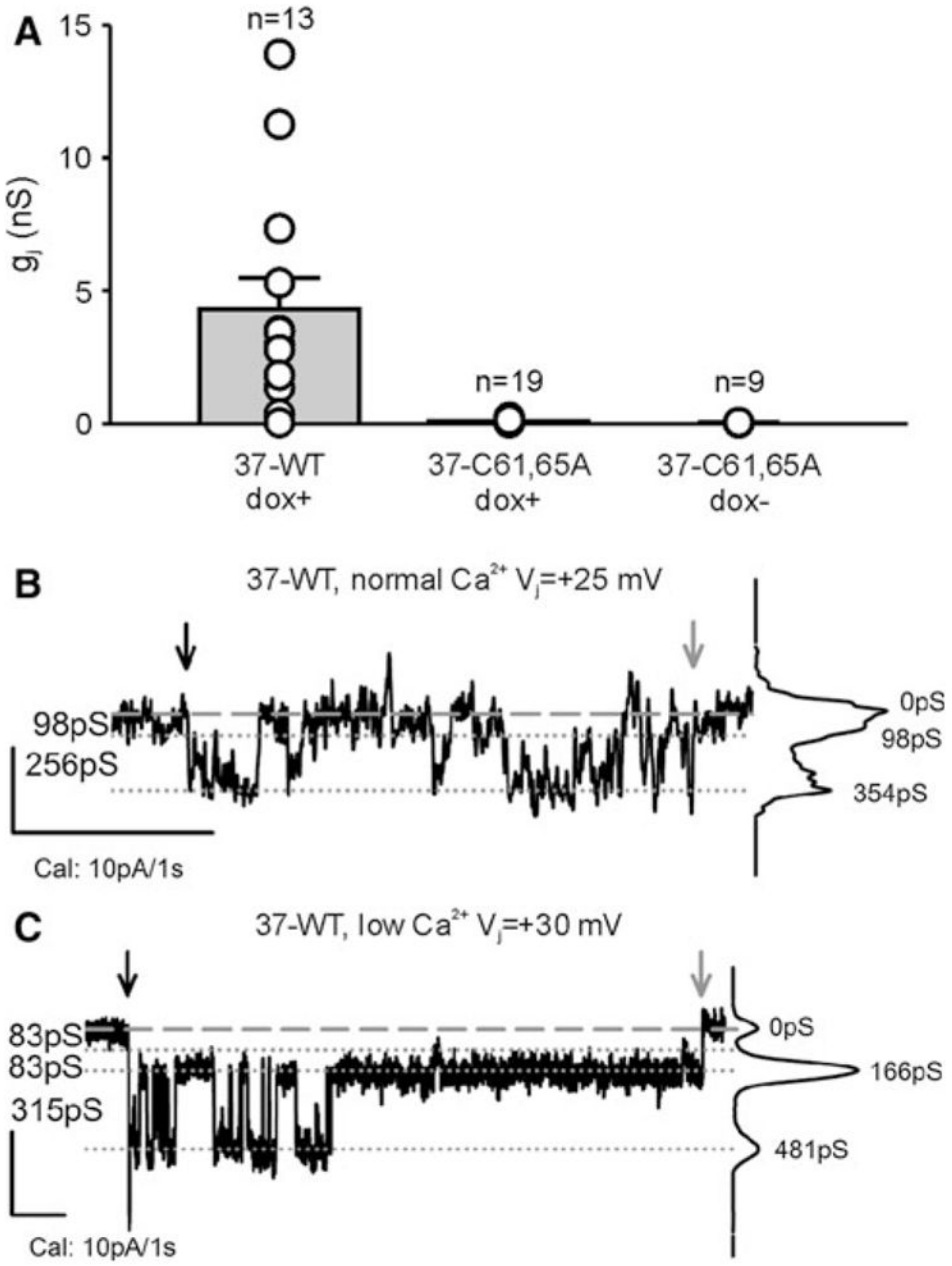

Fig. 4.

Cx37-C61,65A does not form functional gap junction channels. **A** iRin cell pairs induced to express Cx37-WT (37-WT dox+) were variably coupled, with g_j commonly between 1 and 5 nS. In contrast, induced and noninduced iRin37-C61,65A cells were not detectably coupled (data from 1C3 and 1D2 clones). Notice that all of the iRin37-C61,65A cell pairs evaluated, whether induced or noninduced, had g_j values <0.3 nS, which is not different from electrical noise at these recording settings. **B, C** Single-channel events from iRin37 dox+ recorded in external solutions containing either normal (**B**) or low (**C**) calcium, as described in the dye-uptake protocol. Notice that channel flickering decreased upon introduction of low external calcium so that transitions corresponding to ~300 pS and substates corresponding to ~80 pS were readily apparent. *Downward black* and *gray arrows* indicate the start and end of the voltage pulse, respectively

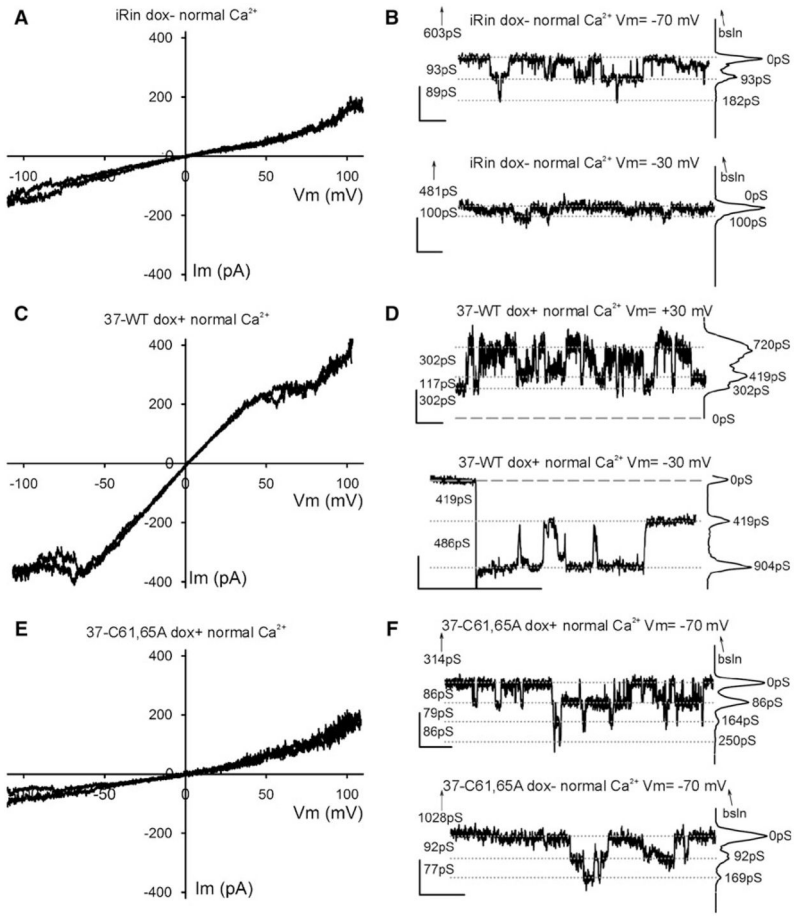

Fig. 5.

Whole-cell voltage-clamp recordings obtained in normal external calcium concentration conditions. **A**, **C**, **E** Plots showing two exemplary traces of voltage ramps applied to parental iRin (not transfected with any Cx37) (**A**), iRin37 (**C**) and iRin37-C61,65A (**E**) cells bathed in solutions with normal external calcium content. In (**C**) the two representative traces were from a series of ten ramps from an iRin37 cell that showed current inactivation at high voltage values. **B**, **F** Transitions of membrane current (corresponding to 85–100 pS) appeared with square V_m pulses in iRin (**B**) and iRin37-C61,65A (**F**) induced (*top trace*) and noninduced (*bottom trace*) cells. Note that these current transitions are barely distinguishable from the noise at $V_m = -30$ mV (**B**, *bottom trace*); however, transitions of similar conductance were also observed at $V_m = -70$ mV. **D** Transitions of membrane current from single cells expressing Cx37-WT during ±30-mV square pulses in normal external calcium. Notice that recording is noisier at positive values; while these are contiguous recordings, transitions appear larger (>400 pS) at negative voltages. **B**, **D**, **F** All-points histograms are shown at the *right* of each trace, baseline is denoted by *dashed lines* and current levels by *dotted lines*, numbers on the *left* correspond to "between lines" conductance differences and numbers next to the histogram peaks indicate the cumulative conductance from the chosen zero current level; *upward-pointing arrows* indicate the distance (in pS) and direction of the true (zero current) baseline, when not displayed; *vertical/horizontal calibration bars* correspond to 10 pA and 1 s, respectively

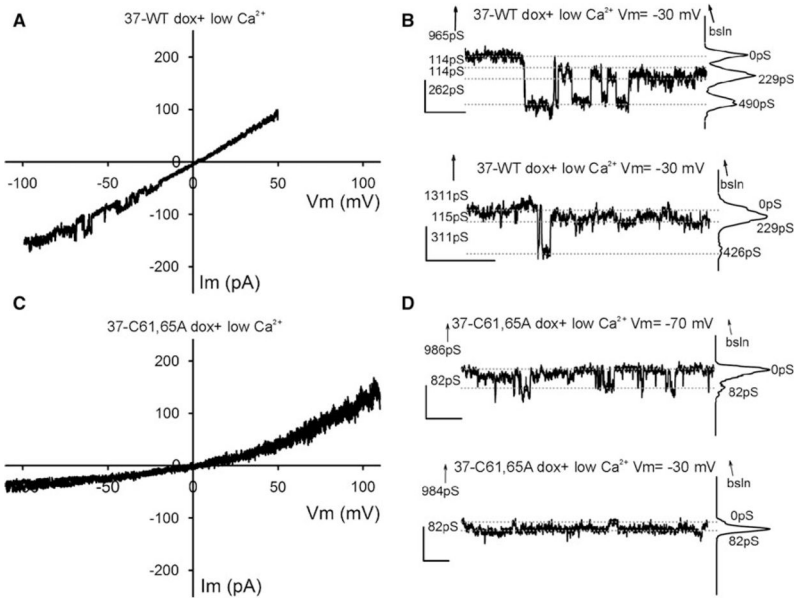

Fig. 6.

Whole-cell voltage-clamp recordings obtained under conditions of low extracellular calcium concentration. **A, C** Plots showing one or two exemplary traces of ramps from iRin37 (**A**) and iRin37-C61,65A (**C**) cells. iRin37 cells (**A**) in low external calcium conditions show clear evidence of channel transitions in the V_m range of −20 to −60 mV (observed in two out of ten ramps, one shown), while Cx37-C61,65A-expressing cells (**c**) show no evidence of channel activity in any ramps in the V_m range −20 to −60 mV (see text for further details). **B** Transitions of membrane current (corresponding to conductances <400 pS) from single cells expressing Cx37-WT during −30 mV square pulses in low external calcium. Notice that most events appear to be smaller than observed in normal calcium, perhaps revealing more transitions to and from a substate. **D** Current transitions of Cx37-C61,65A-expressing cells. Notice transitions correspond to events of less than 100 pS. Traces are labeled as in Fig. 5 *B*, *D* and *F*